

Edge electron states for quasi-one-dimensional organic conductors in the magnetic-field-induced spin-density-wave phases

K. Sengupta, Hyok-Jon Kwon, and Victor M. Yakovenko

Department of Physics and Center for Superconductivity Research, University of Maryland, College Park, MD 20742-4111
(cond-mat/0006050, v.1: June 03, 2000, v.2: January 17, 2001)

We develop a microscopic picture of the electron states localized at the edges perpendicular to the chains in the Bechgaard salts in the quantum Hall regime. In a magnetic-field-induced spin-density-wave state (FISDW) characterized by an integer N , there exist N branches of chiral gapless edge excitations. Localization length is much longer and velocity much lower for these states than for the edge states parallel to the chains. We calculate the contribution of these states to the specific heat and propose a time-of-flight experiment to probe the propagating edge modes directly.

PACS numbers: 74.70Kn, 75.30Fv, 73.40Hm, 73.20-r

Quasi-one-dimensional (Q1D) organic conductors of the (TMTSF)₂X family [1] (also known as the Bechgaard salts) are highly anisotropic crystals that consist of parallel conducting chains. The electron transfer integrals along the chains (in the **a** direction) and transverse to the chains (in the **b** and **c** directions) are $t_a = 250$ meV, $t_b = 25$ meV, and $t_c = 1.5$ meV [2]. Because of the strong Q1D anisotropy, the Fermi surfaces of these materials are open and consist of two disconnected sheets located near $\pm k_F$, which are the Fermi momenta along the chains. In the presence of a strong magnetic field along the **c** axis, the interplay between the nesting property of the open Fermi surface and the quantization of electron orbits due to the magnetic field leads to a cascade of the magnetic-field-induced spin-density-wave (FISDW) phase transitions [2,3]. FISDW opens an energy gap Δ_N in the electron spectrum at the Fermi level. Within each FISDW phase, the Hall conductivity per **a-b** layer per electron spin is quantized at zero temperature as $\sigma_{xy} = Ne^2/h$, where N is an integer that characterizes the FISDW, e is the electron charge, and h is the Planck constant.

The theory of the quantum Hall effect (QHE) in the Bechgaard salts was mostly oriented toward the bulk description [3]. Particularly, the (2+1)D Chern-Simons term has been derived microscopically for the bulk effective action of the system in Ref. [4]. According to general principles [5,6], a system where the Hall effect is quantized with an integer number N should have N gapless chiral electron states at the edges of the sample. However, specific microscopic realization of such edge modes in Q1D organic conductors was not clear. In these systems, the electron states at the edges parallel and perpendicular to the conducting chains must be very different because of the strong anisotropy. The edges parallel to the chains were studied microscopically in Ref. [7]. It was shown, that the $+k_F$ electrons on the first N chains at one edge and the $-k_F$ electrons on the last N chains at the other edge remain ungapped in the FISDW state. The velocity of these chiral modes is equal to the Fermi velocity v_F along the chains. However, the edges per-

pendicular to the chains were not discussed in Ref. [7]. Phenomenological and numerical studies of multilayered quantum Hall systems [8,9] did not address the microscopics and anisotropy of the edge states in Q1D case.

In this letter, we develop a microscopic theory of the chiral states in Q1D conductors at the edges perpendicular to the chains. We find N branches of gapless edge excitations that are localized along the chains within the coherence length $\xi_N = \hbar v_F / \Delta_N$. Their group velocity perpendicular to the chains is $v_\perp = N \Delta_N b / \hbar$, where b is the interchain distance in the **b** direction. Thus, their localization length is much longer and the velocity much lower than the corresponding parameters Nb and v_F for the edge states parallel to the chains.

To explain the origin of the edge states [10], it is useful first to consider a one-dimensional (1D) charge- or spin-density-wave (CDW/SDW) system. The mean-field Hamiltonian for the system can be written as

$$\mathcal{H} = \int dx \psi^\dagger(x) \left(-\frac{\hbar^2 \partial_x^2}{2m} + 2\Delta \cos(2k_F x + \theta) \right) \psi(x), \quad (1)$$

where we have chosen the x axis along the chain. $\psi(x)$ is the fermion (electron) field, m is the effective mass of the fermions, $2\Delta \cos(2k_F x + \theta)$ is the density-wave potential, and θ is the phase specifying the density-wave position. To simplify the presentation, we suppress the spin structure of the fermion field and the order parameter, which is not essential for our purposes. Following the standard procedure, we introduce a doublet of fermion fields, ψ_+ and ψ_- , with momenta close to the Fermi points $\pm k_F$:

$$\psi(x) = \psi_+(x) e^{ik_F x} + \psi_-(x) e^{-ik_F x}, \quad (2)$$

and linearize the energy dispersion relation near the Fermi points. The Hamiltonian can then be written in terms of the fermion doublet $\psi = (\psi_+, \psi_-)$ as

$$\mathcal{H} = \int dx \psi^\dagger(x) (\tau_0 \epsilon_F - \tau_z i \hbar v_F \partial_x + \tau_x \Delta e^{-i\tau_z \theta}) \psi(x), \quad (3)$$

where $v_F = \hbar k_F / m$ is the Fermi velocity, $\epsilon_F = \hbar^2 k_F^2 / 2m$ is the Fermi energy, and τ_x, τ_y, τ_z and τ_0 are the 2×2

Pauli and unit matrices acting on the fermion fields. From Hamiltonian (3), one obtains the eigenvalue equation for the quasiparticles:

$$(-\tau_z i\hbar v_F \partial_x + \tau_x \Delta e^{-i\tau_z \theta}) \psi = E\psi, \quad (4)$$

where E is the quasiparticle energy as measured from the Fermi energy. For an infinite sample, Eq. (4) has well-known plane-wave solutions $\psi \propto e^{ikx}$ with the spectrum

$$E_k = \pm \sqrt{\hbar^2 v_F^2 k^2 + \Delta^2}. \quad (5)$$

The spectrum (5) forbids electron states within the energy gap $\pm\Delta$.

Now let us consider a semi-infinite CDW/SDW system occupying the positive semispace $x > 0$ with an edge at $x = 0$. In this case, the wave function must vanish at the edge: $\psi(x=0) = 0$, or equivalently $\psi_+(x=0) = -\psi_-(x=0)$. With this boundary condition, in addition to the delocalized states (5), Eq. (4) also admits a localized state with the energy $|E| < \Delta$ inside the gap:

$$\psi_{\pm} = \pm e^{-\kappa x} / \sqrt{\kappa}, \quad E = -\Delta \cos \theta, \quad \kappa = -\sin \theta / \xi. \quad (6)$$

The wave function (6) decays in the bulk at a length of the order of the coherence length $\xi = \hbar v_F / \Delta$. Eq. (6) is meaningful only when $\kappa > 0$, thus the localized state exists only for $\pi < \theta < 2\pi$. If the CDW/SDW is displaced by one period, the phase θ changes from 0 to 2π , and the energy of the edge state (6) changes from Δ to $-\Delta$. This process is the spectral flow [11] from the upper to the lower energy band (5). (The opposite spectral flow takes place at the other end of the sample.) The edge state (6) is similar to the electron state localized at the kink soliton in an infinite CDW/SDW system [12].

Now let us consider a Q1D FISDW system. The Hamiltonian of this system differs from Hamiltonian (1) by the interchain tunneling term with the amplitude t_b [3,4]:

$$\mathcal{H}' = \int dx \frac{dk_y}{2\pi} \psi^\dagger(x, k_y) \left(-\frac{\hbar^2 \partial_x^2}{2m} + 2t_b \cos(k_y b - Gx) + 2\Delta \cos(Q_x x + \theta) \right) \psi(x, k_y), \quad (7)$$

where k_y is the electron wave vector transverse to the chains. In the presence of an external magnetic field H , the interchain tunneling term contains the magnetic wave vector $G = ebH/\hbar c$ (c is the speed of light) because of the Peierls-Onsager substitution $k_y - eA_y/c\hbar$ with the vector potential $A_y = Hx$ in the Landau gauge. Another difference between Hamiltonians (1) and (7) is that the FISDW wave vector Q_x deviates from $2k_F$ by an integer multiple N of G : $Q_x = 2k_F - NG$ [3,4]. To simplify presentation, here we neglect the coupling t_c between the (**a-b**) layers and model the system as a set of uncoupled 2D planes. Further, we only consider the electron tunneling between the nearest-neighboring chains and also assume

that the transverse component of the FISDW wave vector is zero. While these assumptions are too simplistic for computation of the quantities such as N , Δ , and T_c , they do not affect our results about the edge states.

Next we introduce the doublet of fermion fields $\psi = (\psi_+, \psi_-)$ as in Eq. (2) and linearize the energy dispersion near $\pm k_F$. The Hamiltonian becomes

$$\mathcal{H}' = \int dx \frac{dk_y}{2\pi} \psi^\dagger(x, k_y) \left(\tau_0 \epsilon_F - \tau_z i\hbar v_F \partial_x + \tau_0 2t_b \cos(k_y b - Gx) + \tau_x \Delta e^{i\tau_z (NGx - \theta)} \right) \psi(x, k_y). \quad (8)$$

Then we make a chiral transformation of the doublet ψ :

$$\psi(x, k_y) = e^{i\tau_z \varphi(x, k_y)} \psi'(x, k_y), \quad (9)$$

$$\varphi(x, k_y) = (2t_b / \hbar \omega_c) \sin(k_y b - Gx), \quad (10)$$

where $\hbar \omega_c = \hbar v_F G$ is the cyclotron energy. In terms of the new field ψ' , the Hamiltonian can be written as

$$\mathcal{H}' = \int dx \frac{dk_y}{2\pi} \psi'^\dagger(x, k_y) \left(\tau_0 \epsilon_F - \tau_z i\hbar v_F \partial_x + \tau_x \Delta e^{i\tau_z [NGx - \theta + 2\varphi(x, k_y)]} \right) \psi'(x, k_y). \quad (11)$$

The transverse hopping term is now transferred to the phase of the FISDW order parameter. Next, we expand that phase factor into a Fourier series

$$e^{2i\tau_z \varphi(x, k_y)} = \sum_n J_n(4t_b / \hbar \omega_c) e^{i\tau_z n(k_y b - Gx)}, \quad (12)$$

where J_n is the Bessel function of the order n . Substituting Eq. (12) into Eq. (11), we only retain the term with $n = N$ in the series, since only this term does not have an oscillatory dependence on x and opens a gap at the Fermi level. This is the so-called single-gap approximation [13,14]. The Hamiltonian then becomes

$$\mathcal{H}' = \int dx \frac{dk_y}{2\pi} \psi'^\dagger(x, k_y) \left(\tau_0 \epsilon_F - \tau_z i\hbar v_F \partial_x + \tau_x \Delta_N e^{i\tau_z (Nk_y b - \theta)} \right) \psi'(x, k_y), \quad (13)$$

where $\Delta_N = \Delta J_N(4t_b / \hbar \omega_c)$ is the modified gap amplitude. Comparing Eqs. (13) and (3), we see that the Q1D FISDW Hamiltonian has been mapped onto an effective 1D CDW/SDW Hamiltonian with the gap amplitude Δ_N and the order-parameter phase $\theta - Nk_y b$.

Now let us consider a semi-infinite FISDW system occupying the positive semispace $x > 0$ along the chains and infinite space in the y -direction transverse to the chains. The wave function ψ' must vanish at the edge: $\psi'_+(0, y) = -\psi'_-(0, y)$. Following the same calculation as for the 1D CDW/SDW, we find the edge states with the energies $|E| < \Delta_N$ inside the gap:

$$\psi'_{\pm}(x, k_y) = \pm e^{ik_y y - \kappa x} / \sqrt{\kappa}, \quad \kappa = \sin(Nk_y b) / \xi_N, \quad (14)$$

$$E_N(k_y) = -\Delta_N \cos(Nk_y b), \quad \xi_N = \hbar v_F / \Delta_N. \quad (15)$$

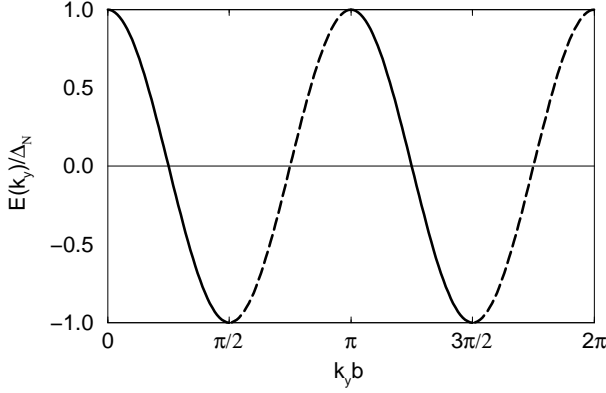


FIG. 1. Energy dispersion of the electron states localized at the left (solid lines) and right (dashed lines) edges of the sample as a function of the transverse momentum k_y for $N = 2$.

Here $E_N(k_y)$ is the quasi-particle energy measured from the Fermi energy, and we have dropped the now unimportant phase θ . The single bound state (6) is now replaced by the band (15) of the edge states labeled by the wave vector k_y perpendicular to the chains. These states (14) are bound along the direction of the chains, but are extended in the direction transverse to the chains. At the left edge of the sample, we require that $\kappa > 0$ and $0 < Nk_y b < \pi$, and find N branches of the edge states in the transverse Brillouin zone $0 < k_y b < 2\pi$. Complementary N branches of the edge states determined by the condition $\kappa < 0$ and $\pi < Nk_y b < 2\pi$ exist at the right edge. The solid and dashed lines in Fig. 1 show the energy dispersions of the states localized at the left and right edges, respectively (for $N = 2$). It is clear that the group velocities of the edge modes $\partial E_N(k_y)/\hbar \partial k_y$ have opposite signs for the left and right edges. Thus, they carry a surface current around the sample, as indicated by the arrows in Fig. 2. The sense of circulation is determined by the sign of N , which is controlled by the sign of the magnetic field H .

An effective action for the low-lying edge excitations can be obtained by linearizing the energy dispersion (15) near the Fermi energy. Since there are N branches of these excitations, the effective action can be written in terms of an N -component chiral fermion field $\phi = (\phi_1, \phi_2, \dots, \phi_N)$, as in Ref. [6]:

$$S_{\text{edge}} = \int dt dy \phi^\dagger(t, y) (i\hbar \partial_t + i\hbar v_\perp \partial_y) \phi(t, y),$$

$$v_\perp = \frac{1}{\hbar} \left(\frac{\partial E_N(k_y)}{\partial k_y} \right)_{E_N(k_y)=0} = \frac{N \Delta_N b}{\hbar}, \quad (16)$$

where t is time. The group velocity v_\perp (16) is same for all branches. The velocity is rather low, because it is proportional to the small FIDSW gap Δ_N . The activation energy $2\Delta_N = 6\text{K}$ was measured in $(\text{TMTSF})_2\text{ClO}_4$ [15] at $H = 25\text{ T}$, where $N = 1$. The BCS relation $\Delta = 1.76 T_c$

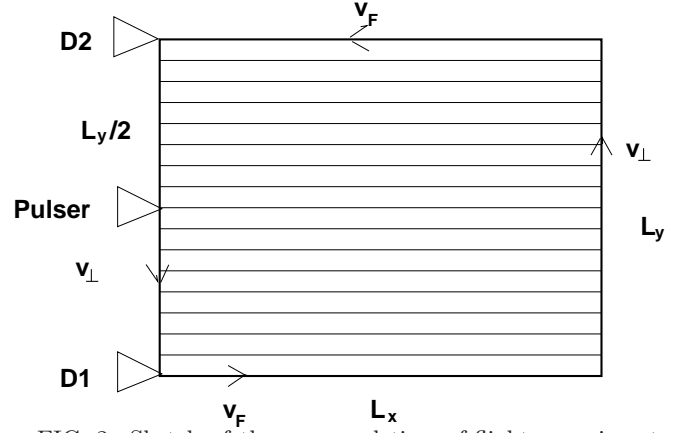


FIG. 2. Sketch of the proposed time-of-flight experiment. The arrows indicate the directions of the edge modes velocities v_\perp and v_F . The thin lines indicate the conducting chains in the sample. The pulser sends a pulse, which is detected at different times t and t' by the detectors D1 and D2.

gives even bigger value $\Delta_N = 5.3\text{ K}$ for $T_c = 3\text{ K}$ at $H = 9\text{ T}$ in $(\text{TMTSF})_2\text{ClO}_4$ [16]. Using the value $\Delta_N = 3\text{ K}$ for $N = 1$, and the lattice spacing $b = 0.77\text{ nm}$, we find $v_\perp = 300\text{ m/s}$. The group velocity for the edges perpendicular to the chains, v_\perp , is three orders of magnitude lower than for the edges parallel to the chains, $v_F = 190\text{ km/s}$ (see Fig. 2). Nevertheless, the total edge current I is the same: $I = (Ne/\pi\hbar) \int_0^{\pi/2bN} (\partial E_N/\partial k_y) dk_y = Ne\Delta_N/\pi\hbar = ev_\perp/\pi b = 20\text{ nA}$. For the typical sample dimensions $L_x = 2\text{ mm}$ and $L_y = L_z = 0.2\text{ mm}$ and the interlayer spacing 1.35 nm , the edge current I produces the magnetic moment 1.2 nA m^2 and magnetization 15 A/m . However, there are additional contributions to the total magnetization coming from the edge states inside the energy gaps opened by the neglected terms in Eq. (12) below the Fermi level [14]. Magnetization has been calculated using the bulk free energy in Ref. [17] and measured experimentally in $(\text{TMTSF})_2\text{ClO}_4$ in Ref. [18].

The gapless edge excitations make a contribution C_e to the specific heat per layer proportional to temperature T at $T \ll \Delta_N$:

$$\frac{C_e}{T} = \frac{N\pi}{3\hbar} \left(\frac{2L_y}{v_\perp} + \frac{2L_x}{v_F} \right) \approx \frac{2\pi}{3\Delta_N} \frac{L_y}{b}. \quad (17)$$

Using the numbers quoted above, we find that $t_x = L_x/v_F = 10\text{ ns}$ and $t_y = L_y/v_\perp = 0.67\text{ }\mu\text{s}$ for $N = 1$. Thus, the dominant contribution to the specific heat comes from the edges perpendicular to the chains. According to Eq. (17), the specific heat must be discontinuous at the boundaries between the FIDSW phases, where Δ_N changes discontinuously [17]. Note that N cancels out in Eq. (17). This result is in contrast with the phenomenological model of Ref. [9], where the edge velocity was assumed to be the same for all FIDSW phases and much stronger discontinuities $C_e/T \sim N$ were predicted.

The bulk specific heat in the normal state is also

proportional to temperature: $C_b^{(n)}/T = \pi L_x L_y / 3\hbar v_F$. Its ratio to the edge specific heat (17) is roughly equal to the ratio of the volumes occupied by the bulk and edge states: $C_b^{(n)}/C_e = L_x/2\xi_N = 2.1 \times 10^3$. In the FISDW phase, the bulk specific heat $C_b^{(F)}/T \approx \sqrt{18/\pi^3} (\Delta_N/T)^{5/2} \exp(-\Delta_N/T) C_b^{(n)}/T$ is smaller than the edge one at the sufficiently low temperature $T \leq \Delta_N/14$. Such a regime could have possibly been achieved at $H = 9$ T in the experimental measurements of the specific heat [16] performed at $T = 0.32$ K in $(\text{TMTSF})_2\text{ClO}_4$. We estimate the absolute values of C_e/T as 2.2×10^{-3} mJ/(K² mole) and $C_b^{(n)}/T$ as 4.4 mJ/(K² mole). The latter estimate roughly matches the experimental value 5 mJ/(K² mole) [16].

The edge states picture was confirmed in a multilayered GaAs system by demonstrating that the conductance G_{zz} perpendicular to the layers is proportional to the number of the edge states N and the perimeter of the sample [19]. A similar experiment on the Bechgaard salts produced inconclusive results [20]. As a definitive proof of the edge states picture for a FISDW, we propose a time-of-flight experiment analogous to those performed on GaAs in Ref. [21]. The experimental setup is sketched in Fig. 2. A pulse is applied by the pulser at the center of the edge perpendicular to the chains. The pulse can be electric, as in Ref. [21], and produce a charge perturbation in the occupation number of the edge states. Alternatively, the pulse can be thermal and perturb the Fermi distribution function of the edge electrons, or magnetic and change the spin population of the edge states [22]. The pulse will travel with the slow velocity v_\perp along the edges perpendicular to the chains and the fast velocity v_F parallel to the chains. The pulse will reach the detector D1 at a time $t = L_y/2v_\perp$ and other detector D2 at a time $t' = 3t + 2L_x/v_F \approx 3t$. The difference between t and t' is a signature of the broken time-reversal symmetry in the system. The inverse delay time $1/t$ is proportional to v_\perp , given by Eq. (16), and has discontinuities at the FISDW phase boundaries due to discontinuity of both N and Δ_N . The pulse must be shorter than $t = 0.33$ μs for clear resolution and longer than $\hbar/\Delta_N = 2.6$ ps, so that only the low-lying excitations are probed.

In conclusion, we have shown, starting from a microscopic Hamiltonian, that there are N chiral gapless electron states bound to the edges perpendicular to the chains in a FISDW phase characterized by an integer N . The gapless modes contribute a term linear in temperature, which dominates the specific heat at low temperatures. The group velocity of these excitations is rather low: $v_\perp = N\Delta_N b/\hbar \approx 300$ m/s. We have proposed a time-of-flight experiment to probe the propagating edge modes directly. The chiral character of these states makes them similar to the edge states in superconductors with broken time-reversal symmetry, such as $d + is$ and $d_{x^2-y^2} + id_{xy}$ singlet superconductors and

$p_x + ip_y$ triplet superconductors Sr_2RuO_4 and 2D $^3\text{He-A}$ [23]. $(\text{TMTSF})_2\text{X}$ in the superconducting state is expected to have nonchiral midgap edge states [24].

-
- [1] TMTSF stands for tetramethyltetraselenafulvalene, and X represents inorganic anions such as ClO_4 or PF_6 .
 - [2] T. Ishiguro, K. Yamaji, and G. Saito, *Organic Superconductors* (Springer, Berlin, 1998).
 - [3] See reviews in the I. F. Schegolev memorial issue J. Phys. (Paris) I **6**, #12 (1996).
 - [4] V. M. Yakovenko and H. S. Goan, Phys. Rev. B **58**, 10648 (1998); V. M. Yakovenko, *ibid.* **43**, 11353 (1991).
 - [5] B. I. Halperin, Phys. Rev. B **25**, 2185 (1982); X. G. Wen, Phys. Rev. Lett. **64**, 2206 (1990); Y. Hatsugai, Phys. Rev. Lett. **71**, 3697 (1993); Phys. Rev. B **48**, 11851 (1993); J. Phys. Cond. Mat. **9**, 2507 (1997);
 - [6] C. L. Kane and M. P. A. Fisher, in *Perspectives in Quantum Hall Effects*, edited by S. Das Sarma and A. Pinczuk (Wiley, New York, 1997), Ch. 4.
 - [7] V. M. Yakovenko and H. S. Goan, J. Phys. (Paris) I **6**, 1917 (1996).
 - [8] J. T. Chalker and A. Dohmen, Phys. Rev. Lett. **75**, 4496 (1995).
 - [9] L. Balents and M. P. A. Fisher, Phys. Rev. Lett. **76**, 2782 (1996).
 - [10] S. G. Davison and M. Stęślička, *Basic Theory of Surface States* (Oxford University Press, Oxford, 1996).
 - [11] M. Stone, Phys. Rev. B **54**, 13222 (1996).
 - [12] S. A. Brazovskii, Zh. Eksp. Teor. Fiz. **78**, 677 (1980) [Sov. Phys. JETP **51**, 342 (1980)].
 - [13] D. Poilblanc, M. Héritier, G. Montambaux and P. Lederer, J. Phys. C **19**, L321 (1986); A. Virosztek, L. Chen, and K. Maki, Phys. Rev. B **34**, 3371 (1986).
 - [14] The single-gap approximation is not sufficient for self-consistent calculation of thermodynamic quantities, such as free energy and magnetization [17]. However, it is adequate for describing the low-energy electron states inside the gap at the Fermi level in the case $\Delta \ll \hbar\omega_c$ [4,7]. It fits the temperature dependence of the Hall effect very well: see T. Vuletić *et al.*, cond-mat/0010106.
 - [15] R. V. Chamberlin *et al.*, Synth. Met. **27**, B 41 (1988).
 - [16] U. M. Scheven *et al.*, Phys. Rev. B **52**, 3484 (1995).
 - [17] G. Montambaux and D. Poilblanc, Phys. Rev. B **37**, 1913 (1988); G. Montambaux *et al.*, *ibid.* **39**, 885 (1989).
 - [18] M. J. Naughton *et al.* Phys. Rev. Lett. **55**, 969 (1985).
 - [19] D. P. Druist *et al.*, Phys. Rev. Lett. **80**, 365 (1998).
 - [20] S. Uji *et al.*, Phys. Rev. B **60**, 1650 (1999).
 - [21] R. C. Ashoori *et al.*, Phys. Rev. B **45**, 3894 (1992); G. Ernst *et al.*, Phys. Rev. Lett. **79**, 3748 (1997).
 - [22] J. M. Kikkawa and D. D. Awschalom, Nature **397**, 139 (1999).
 - [23] T. Senthil, J. B. Marston, and M. P. A. Fisher, Phys. Rev. B **60**, 4245 (1999); C. Honerkamp and M. Sigrist, J. Low T. Phys. **111**, 895 (1998); G. E. Volovik, Pis'ma Zh. Eksp. Teor. Fiz. **55**, 363 (1992) [JETP Lett. **55**, 368 (1992)].
 - [24] K. Sengupta *et al.*, cond-mat/0010206.